Published online 30 April 2016

Nucleic Acids Research, 2016, Vol. 44, No. 13 ***6409–6422***
doi: 10.1093/nar/gkw338

Loss of the mitochondrial protein-only ribonuclease P complex causes aberrant tRNA processing and lethality in Drosophila

Aditya Sen[1,†], Agnes Karasik[1,†], Aranganathan Shanmuganathan[1], Elena Mirkovic[2], Markos Koutmos[1,*] and Rachel T. Cox[1,*]

[1]Department of Biochemistry and Molecular Biology, Uniformed Services University, Bethesda, MD, 20814, USA and [2]Walt Whitman High School, Bethesda, MD, 20817, USA

Received February 26, 2016; Revised April 12, 2016; Accepted April 14, 2016

ABSTRACT

Proteins encoded by mitochondrial DNA are translated using mitochondrially encoded tRNAs and rRNAs. As with nuclear encoded tRNAs, mitochondrial tRNAs must be processed to become fully functional. The mitochondrial form of ribonuclease P (mt:RNase P) is responsible for 5′-end maturation and is comprised of three proteins; mitochondrial RNase P protein (MRPP) 1 and 2 together with proteinaceous RNase P (PRORP). However, its mechanism and impact on development is not yet known. Using homology searches, we have identified the three proteins composing Drosophila mt:RNase P: Mulder (PRORP), Scully (MRPP2) and Roswell (MRPP1). Here, we show that each protein is essential and localizes with mitochondria. Furthermore, reducing levels of each causes mitochondrial deficits, which appear to be due at least in part to defective mitochondrial tRNA processing. Overexpressing two members of the complex, Mulder and Roswell, is also lethal, and in the case of Mulder, causes abnormal mitochondrial morphology. These data are the first evidence that defective mt:RNase P causes mitochondrial dysfunction, lethality and aberrant mitochondrial tRNA processing *in vivo*, underscoring its physiological importance. This *in vivo* mt:RNase P model will advance our understanding of how loss of mitochondrial tRNA processing causes tissue failure, an important aspect of human mitochondrial disease.

INTRODUCTION

Most metazoan mitochondrial genomes encode the same transcripts (1). The 13 proteins encoded by mitochondrial DNA (mtDNA) are required components of the complexes that carry out oxidative phosphorylation. In order for mitochondria to fulfill the ATP demands of the cell, each mitochondrial-encoded protein must be efficiently generated by the mitochondrial machinery. To this end, the mitochondrial ribosomes rely on the large and small ribosomal RNAs and the entire suite of tRNAs encoded by the mtDNA.

Nuclear tRNAs are transcribed as pre-tRNAs that require 5′- and 3′-end cleavage and other modifications in order to mature and become fully functional (2–4). As mitochondria have a bacterial origin, mtDNA is transcribed as polycistrons that must be processed and cleaved to create the final products (5,6). Thus, mtDNA transcription is complex and places unique demands on the mitochondrial RNA processing machinery, differing significantly from the transcription that commonly takes place in the nucleus (7). Mitochondrial tRNAs (mt:tRNAs) punctuate the mRNAs and rRNAs found in mtDNA and thus have the added complication of requiring excision from the polycistron before maturation (8). In the nucleus, the RNAse P ribozyme has long been known to be responsible for the 5′-end pre-tRNA cleavage reaction, while other endonucleases, such as RNase Z and Rex1p carrying out the 3′-end cleavage reaction (9–11). Recently, a new class of protein-only RNase Ps (proteinaceous RNase P (PRORP)) has been identified that can carry out the 5′-end cleavage in human mitochondria (12). In contrast to the RNAse P ribozyme, PRORP (also called Mitochondrial RNase P Protein 3 (MRPP3)) is a metallonuclease without an RNA component. Single protein PRORPs exist in the nucleus and organelles of land plants and unicellular eukaryotes (13,14). In contrast, human PRORP has only been identified in mitochondria and is part of a three-protein complex referred to as mt:RNase P, comprising mitochondrial RNase P Protein 1 (MRPP1/TRMT10C) and mitochondrial RNase P Protein 2 (MRPP2/SDR5C1/HSD10) (12). MRPP1 is re-

*To whom correspondence should be addressed. Tel: +1 301 295 9791; Fax: +1 301 295 3512; Email: rachel.cox@usuhs.edu
Correspondence may also be addressed to Markos Koutmos. Tel: +1 301 295 9419; Fax: +1 301 295 3512; Email: markos.koutmos@usuhs.edu
†These authors contributed equally to the paper as first authors.

quired for methylation of the ninth position of certain mitochondrial tRNAs, although this activity is not obligatory for mt:RNAse P function and 5′-end cleavage (15). MRPP2 is a dehydrogenase, however evidence supports that in the context of mt:RNase P it is required for the methyltransferase activity of MRPP1, as well as likely functions as a scaffold protein for the formation of an MRPP1 and 2 sub-complex (15). As such, the MRPP1 and MRPP2 subcomplex catalyzes tRNA methylation and in the context of mt:RNase P supports 5′-end processing by PRORP. The 3′-end cleavage of mt:tRNAs also uses a mitochondrially localized RNase Z, called ELAC2 in humans and RNase Z^L in Drosophila. While these two enzyme complexes are distinct, there is evidence that RNase Z/ELAC2 preferentially cleaves products that have already been processed by RNase P (16).

While this newly identified mt:RNAse P complex appears critical for tRNA processing and maturation, it is currently unknown how loss of mt:RNAse P function affects mitochondrial output and health. This is particularly relevant to human health as the majority of mitochondrial diseases caused by mutations in mtDNA are due to point mutations in mt:tRNAs (17). Based on their location, most of the mitochondrial tRNA mutations could affect mt:RNAse P function, leading to unprocessed RNA species and mitochondrial dysfunction. Specific examples include MELAS (mitochondrial encephalopathy, lactic acidosis and stroke-like episodes), mitochondrial myopathy and HSD10 disease (18–23). Highlighting the importance of mt:tRNA processing in human health, mutations in RNase Z/ELAC2 and MRPP2/SDR5C1 are associated with cardiomyopathy and neurodegeneration, and cause mis-regulated mt:tRNA cleavage in cell culture (24,25). For unknown reasons mitochondrial diseases manifest very differently in different organs and tissues and have quite different etiology, making their diagnoses and treatment difficult, therefore it is critical to understand the molecular mechanisms underlying mt:tRNA cleavage *in vivo* (17,26).

Drosophila is an excellent model system to study the effect of altered mtDNA post-transcriptional processes as Drosophila and human mtDNA genomes are arranged in a similar manner, with mt:tRNAs punctuating the mRNAs and rRNAs (27). In order to determine the developmental and physiological significance of mt:RNase P function, we have used sequence similarities to identify the Drosophila mt:RNase P complex and examined Drosophila lacking the orthologs for PRORP, MRPP2 and MRPP1, called Mulder, Scully and Roswell, respectively. Here we show that Mulder, Scully and Roswell localize to mitochondria as expected and that each can associate with the others. Importantly, reducing any one of the three causes lethality. Furthermore, flies lacking Mulder, Scully or Roswell have associated mitochondrial deficiencies, exhibiting greatly reduced levels of ATP and swollen, damaged-looking mitochondria. In addition, flies with reduced Mulder, Scully or Roswell accumulate unprocessed mt:tRNA indicating that the mitochondrial defects we observe are at least in part direct and specific for the protein complex function. Finally, we find that overexpressing either Mulder or Roswell exerts dominant negative effects on development and can also cause mitochondrial defects. These data are the first to show that loss of mt:RNase P function is detrimental in metazoans and specifically mis-regulates mt:tRNA processing. Understanding the role of the highly conserved mt:RNase P will be useful to dissect a subset of the complex mechanisms underlying mitochondrial diseases.

MATERIALS AND METHODS

Fly stocks

The following fly stocks were obtained from the Bloomington Stock Center: y^1 *w* mldr*^{B} FRT19A/FM7i, ActGFP, y^1 *w* mldr*^{C} FRT19A/FM7i, ActGFP, y^1 *w* scu*^{A} FRT19A/FM7i, ActGFP, y^1 *w* scu*^{D} FRT19A/FM7i, ActGFP, y^1 v^1; *scu*$^{TRiP.HMS02305}$, y^1 *sc** v^1; *scu*$^{TRiP.GL01079}$, y^1 *sc** v^1; *rswl*$^{TRiP.HMC02423}$, y^1 *w**; P{w[+mC] = tubP-GAL4}LL7/ TM3, P{w[+mC] = ActGFP}JMR2, Ser[1], y^1 *w**; P{w[+mC] = Act5C-GAL4}17bFO1/ TM3, P{w[+mC] = ActGFP}JMR2, Ser, *w**; P{w[+mC] = ple-GAL4.F}3, P{w[+mC] = GAL4::VP16-nos.UTR}. The following stocks were obtained from the Vienna Drosophila Research Center: *y* w^{1118}/ *mldr*^{KK108043}, w^{1118}; *rswl* ^{GD12447} (28).

Transgenic flies and constructs

The full-length Open Reading Frames for each respective gene was amplified from the following Drosophila ESTs (Drosophila Genomics Resource Center, Bloomington, IN, USA): *rswl* (LD44982), *scu* (IP05285) and *mldr* (SD17694). The two point mutations present in SD17694 were corrected (R250L and L528M) using the QuikChange method (Stratagene). For transgenic flies, *rswl*, *scu* and *mldr* were sub-cloned into pPWM, pPWF and pPWV plasmids (The Drosophila Gateway Collection, Carnegie Institution of Washington, Baltimore, MD, USA), respectively, then commercially injected (Genetic Services, Inc, Cambridge, MA, USA). For S2R+ tissue culture constructs, *rswl*, *scu* and *mldr* were sub-cloned into pAWM containing a C-terminal myc tag. *scu* and *mldr* were also cloned into pAWF containing a C-terminal FLAG tag (The Drosophila Gateway Collection, Carnegie Institution of Washington, Baltimore, MD, USA).

Northern blots

Total RNA was extracted from 5 to 10 mg of wild-type and mutant strains of Drosophila larvae using a Tissue and Insect RNA kit (Zymo Research Corporation, St. Louis, MO, USA). Five micrograms from each sample were mixed with an equal amount of 2× urea loading dye (0.05% Bromo-Phenol-Blue, 0.05% Xylene Cyanol dye, 50% m/v urea, 0.1 M EDTA) and run on 6% urea-polyacrylamide gel. Northern blot analysis was performed according to the DIG Northern Starter Kit (Sigma-Aldrich Corp. St. Louis, MO, USA) with a hybridization temperature of 50°C. The size standards of the RNA fragments were detected using DIG-labeled RNA Molecular Weight Marker I (Sigma-Aldrich Corp. St. Louis, MO, USA). Each blot was performed at least three times.

Immunofluorescence

Larval brains and ovaries from well-fattened females were dissected and fixed as previously described (29). S2R+ culture cells were fixed and mounted as described (29). In short, samples were fixed in Grace's Insect Medium (modified) (BioWhittaker, Lonza, Cologne, Germany) containing 4% paraformaldehyde and 20 mM formic acid (Sigma-Aldrich Corp. St. Louis, MO, USA). Antibody staining was performed in antibody wash buffer (1× PBS:0.1% Triton X-100:1% BSA). The following antibodies were used: rabbit anti-GFP (1:2000, Torrey Pines Biolabs, Secaucus, NJ, USA), mouse anti-myc (1:1000, Sigma-Aldrich Corp. St. Louis, MO, USA), anti-FLAG (1:1000, Sigma-Aldrich Corp. St. Louis, MO, USA), mouse anti-ATP synthase (1:1000, CVA, Mitosciences) and Phalloidin (1:250, Invitrogen). The following secondary antibodies were used: goat anti-mouse $IgG2_b$ Alexa 488, goat anti-mouse $IgG2_b$ Alexa 568, goat anti-mouse IgG_1 Alexa 488 and goat anti-rabbit Alexa 488 (Molecular Probes, Lifetechnologies, Grand Island, NY, USA). Images were collected using Zeiss 710 and Zeiss 700 confocal microscopes and 63× Plan Apo NA 1.4 lens.

Western blotting, immunoprecipitation and cell fractionation

Western blotting, immunoprecipitations (IP) and cell fractionations have been performed as described earlier (29,30). The following antibodies were used: mouse anti-myc (1:5000, Sigma-Aldrich Corp. St. Louis, MO, USA), anti-FLAG (1:10000, Sigma-Aldrich Corp. St. Louis, MO, USA), anti-CVA (1:100000, Mitosciences), mouse anti-alpha tubulin (1:5000, Developmental Studies Hybridoma Bank, University of Iowa, Iowa City, IA, USA) and anti-Mldr (1:2000, this study).

Pupation, eclosion and negative geotaxis measurements

Pupation, eclosion and negative geotaxis measurement were performed as described (29,30). *P*-values were calculated in Microsoft Excel using a two-tailed Student's *t*-test.

ATP measurements and aconitase assay

ATP measurements and aconitase assays were performed as described (29). In short, for ATP measurement, larval samples were homogenized in ATP extraction buffer (100 mM Tris-Cl, pH 8.0, 4 mM EDTA, pH 8.0; 6 M guanidine hydrochloride) and protein concentrations were measured using Bradford assay. The ATP concentration was determined using an ATP Determination Kit (Molecular Probes, Invitrogen) according to the manufacturer's directions. One hundred microliter assays were performed in a 96-well plate and the luminescence was measured using a Biotek Synergy H1 luminometer. Each sample was processed in duplicate and read in triplicate. The amount of ATP was normalized against protein concentration. For aconitase assays, larval extracts were electrophoresed on cellulose acetate membrane (Cellogel, Accurate Chemicals, Westbury, NY, USA) in running buffer [20 mM potassium phosphate (pH 7.8), 3.6 mM citrate]. Aconitase activities were detected on the membrane by incubating it in staining solution [100 mM potassium phosphate, (pH 6.5), 1 mM $NADP_1$, 25 mM $MgCl_2$, 2 mM cis-aconitic acid, 0.5 mg/ml 2,3-bis-(2-methoxy-4-nitro-5-sulfenyl)-2H-tetrazolium-5 carboxanilide disodium salt (XTT) or MTT, 0.3 mM phenazine methosulfate, 5 units/ml isocitrate dehydrogenase] for 10 min. From three membranes, the band intensities from mitochondrial aconitase activity of each sample were normalized against the respective cytoplasmic aconitase activity for comparison. Analyses were done using ImageJ (31).

Mulder antibody generation

The Drosophila EST SD17694 (Drosophila Genomics Resource Center, Bloomington, IN, USA) was cloned into pMCSG7 vector (gifted from Midwest Center for Structural Genomics, IL, USA) and transformed into BL21(DE3) expression cells (New England Biolabs, MA, USA). The culture was grown at 37°C and the protein was expressed using 200 μM of IPTG at 18°C in TB media (Sigma-Aldrich Corp. St. Louis, MO, USA). The cells were lysed using lysis buffer (8M urea, 100 mM NaH_2PO_4, 10 mM Tris and 10 mM imidiazole pH 8.0) and sonication. The lysate was centrifuged and the supernatant was passed through Ni-NTA column and washed with a denaturing wash buffer (8M urea, 100 mM NaH_2PO_4, 150 mM NaCl, 20 mM imidiazole pH 8.0). The protein samples were eluted from the column using 20 mM MOPS pH 7.8,100 mM NaCl, 1 mM TCEP, 500 mM imidazole and 6 M urea. The purity of the sample was verified by SDS PAGE gel and fractions having a single band were pooled and then commercially injected into rabbits (Covance Research Products, Princeton, NJ, USA). A 1 mg/ml protein was used for the injection and the serum was checked by ELISA test for antibody tightness.

RESULTS

Members of the protein only RNase P complex localize to mitochondria in Drosophila

Pre-tRNAs are processed through cleavage of their 5′ and 3′ ends, as well as by the covalent modification of various bases (2,3). In metazoan mitochondria, the protein in the mt:RNase P complex responsible for catalyzing the 5′-end cleavage is PRORP which contains a metallonuclease domain, as well as a pentatricopeptide repeat (PPR) domain thought to bind RNA (Figure 1A). The Drosophila ortholog contains all of the same recognizable domains, including a mitochondrial targeting signal. The Drosophila PRORP ortholog is the previously undescribed gene CG15896 that we have named *mulder* (*mldr*) (Figure 1A). MRPP2 is a member of the short-chain dehydrogenase/reductase (SDR) superfamily and is also known as Hydroxysteroid (17-Beta) Dehydrogenase 10 (HSD10 is the protein, HSD17B10 is the gene) (Figure 1A). The Drosophila ortholog Scully (Scu) is highly homologous to MRPP2, with 69% amino acid identity (Figure 1A) (32). MRPP1 is a methyltransferase and Drosophila contain two potential orthologs. However, only one has a mitochondrial targeting signal, which is encoded by the previously undescribed gene CG5190 that we have named *roswell* (*rswl*) (Figure 1A).

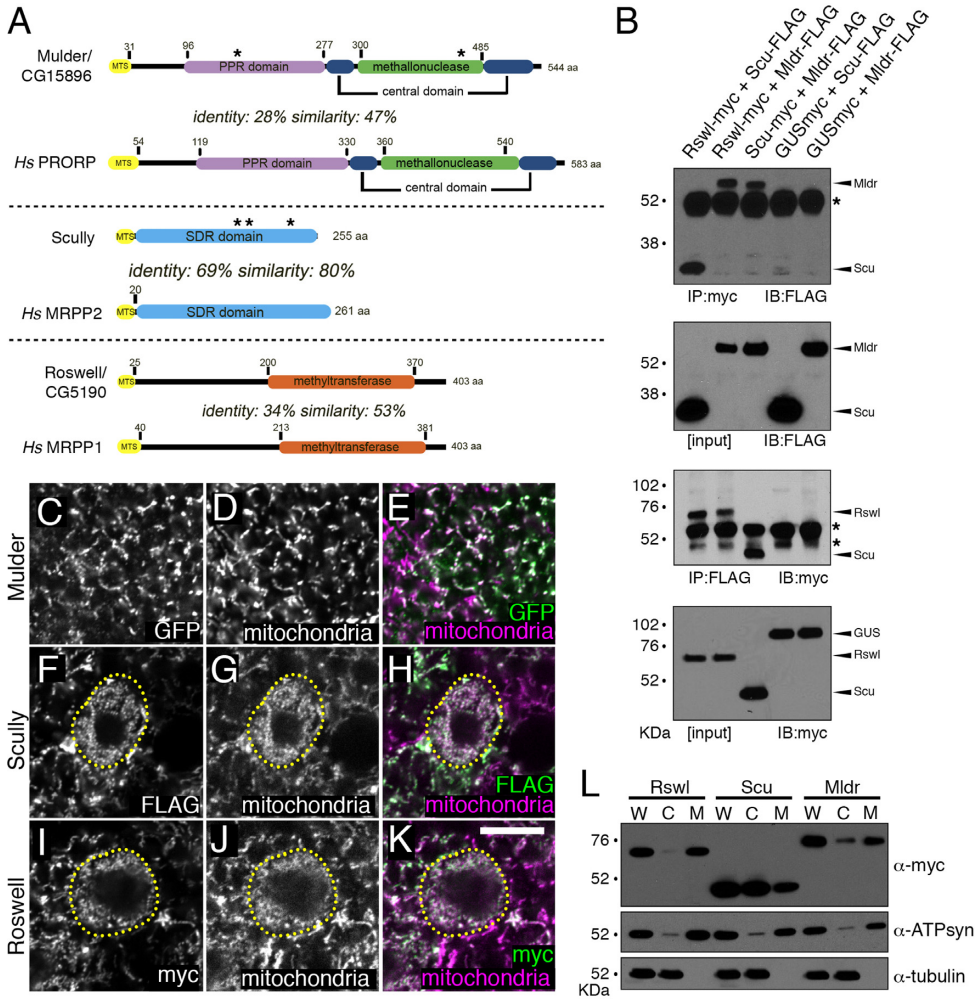

Figure 1. The Drosophila mt:RNase P proteins Mldr, Scu and Rswl localize to mitochondria. (**A**) Schematics indicating the domains of each protein and their homology to the human homologs. Asterisks indicate the approximate location of the mutations used in this study. The length of the mitochondrial targeting sequence (MTS, yellow) was predicted using the Mitoprot server. Domain boundaries of Drosophila mt:RNase P components were predicted based on alignments with human homologs (Clustal Omega). Sequence identify and similarity were determined by BLAST. (**B**) Western blots showing each mt:RNase P protein can reciprocally co-immunoprecipitate with the others. GUS = glucuronidase as a negative control. Arrowheads indicate the correct band size. Asterisks indicate the anti-mouse IgG cross-reactive bands. (**C–K**) GFP-tagged Mldr, FLAG-tagged Scu and myc-tagged Rswl (C, F, I, respectively) co-localize with mitochondria (D, G, J) in larval brains. E, H, K show the merged images. Dashed yellow lines indicate third larval instar neuroblasts. Overexpression of Mldr causes early larval lethality and it is difficult to find NBs in the very young brains, thus there is no NB indicated (C, D). (L) Western blot of fractionated S2R+ cell extract from cells transfected with myc-tagged Mldr, Scu or Rswl shows each protein is located in the mitochondrial fraction (M). Tubulin and ATP synthase are controls for cytoplasmic (C) and mitochondrial (M) fractions, respectively. W = whole cell extract. White = anti-ATP synthase (D, G, J), anti-GFP (C), anti-FLAG (F), anti-myc (I). Green = anti-GFP (E), anti-FLAG (H), anti-myc (K). Magenta = anti-ATP synthase (E, H, K). Scale bar = 10 μm in K for C–K.

For Mldr, Scu and Rswl to exert their function as the Drosophila mt:RNase P, they would have to associate with each other. To test this, we transfected S2R+ cells pairwise with myc- and FLAG-tagged constructs and performed reciprocal immunoprecipitation (IP) (Figure 1B). Rswl and Scu, Rswl and Mldr and Scu and Mldr reciprocally co-IP'd, indicating that the three were able to associate. Myc-tagged glucuronidase (GUS) served as a negative control. Furthermore, the mt:RNase P complex must localize to mitochondria in order to process mt-tRNAs. Mldr, Scu and Rswl contain putative mitochondrial targeting signals (Figure 1A; MTS), however none have been previously shown to localize to mitochondria *in vivo*. To test the localization of each protein, we developed transgenic flies using the UAS/GAL4 system to conditionally express GFP-tagged Mldr, FLAG-tagged Scu and myc-tagged Rswl (33). As evidenced by immunofluorescence, all three proteins co-localized with mitochondrial ATP synthase in the larval brain (Figure 1C–K) and germ cells (Supplementary Figure S1A–F, Figure 6D–F). S2R+ cells transfected with myc-tagged Mldr, Scu and Rswl also showed strong mitochondrial co-localization with ATP synthase (Supplementary Figure S1G–O). To confirm this localization biochemically, we transfected S2R+ cells with myc-tagged Mldr, Scu and Rswl and separated the extract into cytoplasmic and mitochondrial fractions. By probing the fractions with anti-myc antibody, we saw that each protein is detected in the mitochondrial fraction (Figure 1L). There were minimal

amounts of Mldr and Rswl in the cytoplasmic fractions which were likely due to a trace contamination from the mitochondrial fraction judging from the ATP synthase antibody. While immunofluorescence *in situ* showed predominantly mitochondrial staining, Scu was also found in the cytoplasmic fraction, which could be due to overexpression in S2R+ cells that often led to large cytoplasmic aggregates (Supplementary Figure S2, arrows). ATP synthase and tubulin served as controls for the purity of the mitochondrial and cytoplasmic fractions, respectively. Taken together, these data show that Mldr, Scu and Rswl can associate with each other, and that each is localized to mitochondria *in vivo*.

Mulder, Scully and Roswell are orthologous to PRORP, MRPP2 and MRPP1

There are no available structures for Mldr and Scu. We have, however, used known structures of homologous proteins to construct the high confidence models shown in Figure 2. Specifically, Phyre server was used to create a structure model of Mldr using the metallonuclease domain of human PRORP and the full-length structures of A. thaliana PRORP1 and PRORP2 as templates (34–36). The I-Tasser server was used to create a structure model of Scu based on structures of human MRPP2 (37,38). There are two uncharacterized publicly available alleles of *mldr* that were generated in a large-scale mutagenesis screen: $mldr^{B}$ (Y121D in the PPR domain) and $mldr^{C}$ (W465R in the metallonuclease domain) (Figure 2A, yellow circles) (39). There are three available *scu* alleles. Two of them were generated in the same genetic screen as was *mldr*: scu^{D} (S163F) is in a highly conserved residue (Figure 2B, red circle) and scu^{A} (Q159Stop) is predicted to result in a C-terminal truncation (Figure 2B, shown in yellow) (39). scu^{4058} results from a small X-ray induced deletion which causes a frameshift at E205 leading to a stop codon 60 nucleotides downstream after E236 (32). This results in a smaller truncation than scu^{A}, consisting of the last 19 residues (Figure 2B, shown in green). The putative tetrameric assembly of Scu is presented where the four monomers are differentially color-coded (Figure 2C). It is evident that S163 lies in the interface between two monomers.

Reducing Mldr, Scu and Rswl causes lethality *in vivo*

In order to study the consequences of loss of mt:RNase P *in vivo*, we examined mutants for *mldr* and *scu*, and *RNAi* knockdown for *mldr*, *scu* and *rswl*. We found the mutant alleles for *mldr* and *scu* cause lethality because flies containing mutations in either gene do not make it to the adult stage as we only saw heterozygous sibling adult flies eclose, whereas homozygous mutant adults never eclosed (Figure 2D). While $mldr^{B}$ and $mldr^{C}$ are only point mutations, the larvae contained very low protein levels as judged by western blot (Figure 2E). To determine at which stage of development the lethality occurs, we transferred 20 one-day-old mutant larvae into vials and scored how many pupated (Figure 2F–H). Under these uncrowded conditions, $mldr^{B}$ showed a delay in pupation relative to wild-type sibling controls, with all the larvae finally pupating by day 16 (Figure 2F). $mldr^{C}$ had a stronger phenotype, with a longer pupation delay and only 60% of the larvae pupating compared with sibling controls (Figure 2F). The three available *scu* alleles gave similar results. scu^{A} and scu^{D} were both lethal and experienced delayed pupation under uncrowded conditions (Figure 2G). scu^{4058} was the most severe, with a slightly longer pupation delay and only 60% of the larvae pupating (Figure 2G). Pupae mutant for *mldr* and *scu* frequently did not develop normally and had reduced spiracle eversion (Supplementary Figure S3). Expressing *UAS-rswl-RNAi* also gave a modest delay in pupation compared to control (Figure 2H).

In addition to examining both *mldr* and *scu* mutants, we ubiquitously expressed available RNAi lines using the highly expressed *tubGAL4* and lower expressed *ActGAL4* (Table 1 & Supplementary Table S1). Expressing *UAS-scu* and *UAS-mldr RNAi* using *tubGAL4* allowed larvae to pupate equally well as controls. The *scu RNAi* knockdown pupae did not develop to adulthood. Approximately 10% of the *mldr* knockdown pupae eclosed and using ActGAL4 to express the *RNAi* at lower levels allowed an even larger portion of the adults to eclose (Table 1 and Supplementary Table S1). At present, there are no available alleles for *rswl* and only one RNAi stock. Expressing *rswl-RNAi* using *ActGAL4* allowed the larvae to pupate, but not develop. While this is only one RNAi line, this result is very similar to our results with *mldr* and *scu*. Expressing *UAS-rswl* RNAi at higher levels using *tubGAL4* suppressed even pupation (Table 1).

Neurons are particularly sensitive to mitochondrial output. To determine if decreasing Mldr, Scu or Rswl caused neuronal deficits, we expressed *UAS-RNAi* for each using the tyrosine hydroxylase *pleGAL4* specific to dopaminergic neurons and examined the ability of the flies to climb at different ages (Figure 2I). Expressing neither *UAS-rswl* nor *UAS-scu* RNAi caused deficits in locomotion. However, knocking down *mldr* in dopaminergic neurons caused an age-progressive loss of locomotive function (Figure 2I). Taken together, these data support an essential role for mt:RNase P *in vivo*. Furthermore, ubiquitously knocking down each complex member caused lethality at the same developmental stage and thus gave very similar phenotypes, suggesting they function in the same pathway.

mldr and *scu* mutants and *rswl* knockdown larvae have reduced ATP levels but no apparent mitochondrial oxidative stress

In metazoans, mtDNA encodes the entire suite of tRNAs necessary for translating mtDNA encoded proteins. There are only 13 proteins encoded by mtDNA, all of which are required for the protein complexes used for oxidative phosphorylation. Since human mt:RNase P is involved in mt:tRNA processing *in vitro*, we tested whether knocking down each component caused ATP levels to decrease *in vivo*. Larvae mutant for *mldr* and *scu* showed greatly reduced ATP levels relative to wild-type control (Figure 3A). Consistent with this result, extract from larvae expressing *UAS-RNAi* for *mldr*, *scu* and *rswl* also showed low levels of ATP relative to control (Figure 3B). One of the consequences of electron transport during respiration can be the accumula-

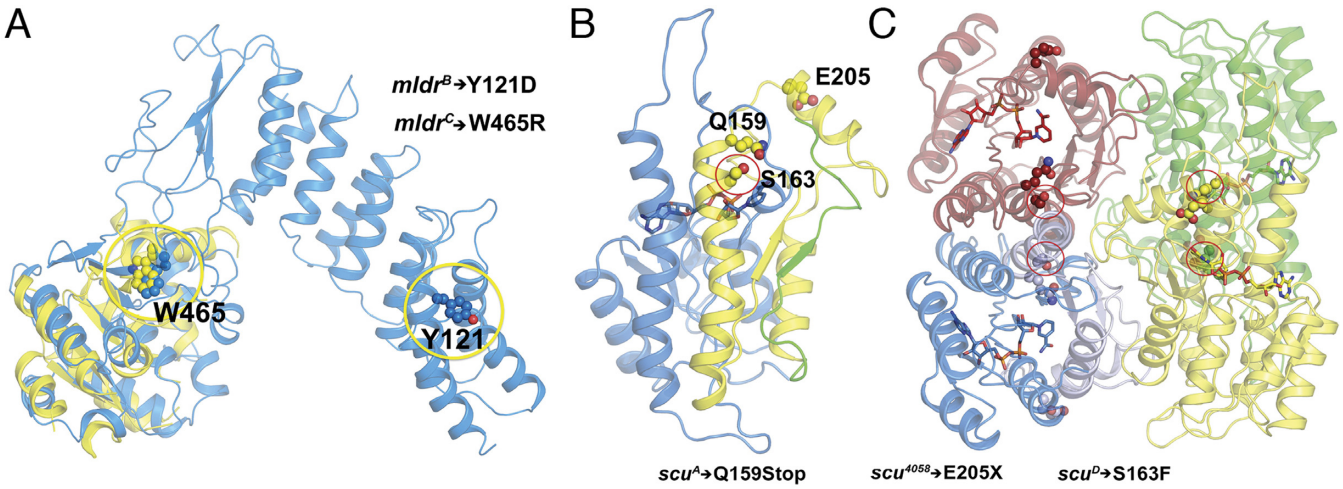

D

	Mutant		Sibling control[a]	
	% pupation*	% eclosion	% pupation	% eclosion
$mldr^B$	92 ± 2.0	0	90 ± 2.6	96 ± 2.0
$mldr^C$	60 ± 5.0	0	87 ± 3.4	98 ± 2.2
scu^A	95 ± 0.0	0	80 ± 2.4	92 ± 5.1
scu^D	90 ± 10	0	86 ± 2.4	96 ± 3.5
scu^{4058}	60 ± 2.9	0	78 ± 9.3	94 ± 5.5

*± s.e.m. [a] GFP+ sibling

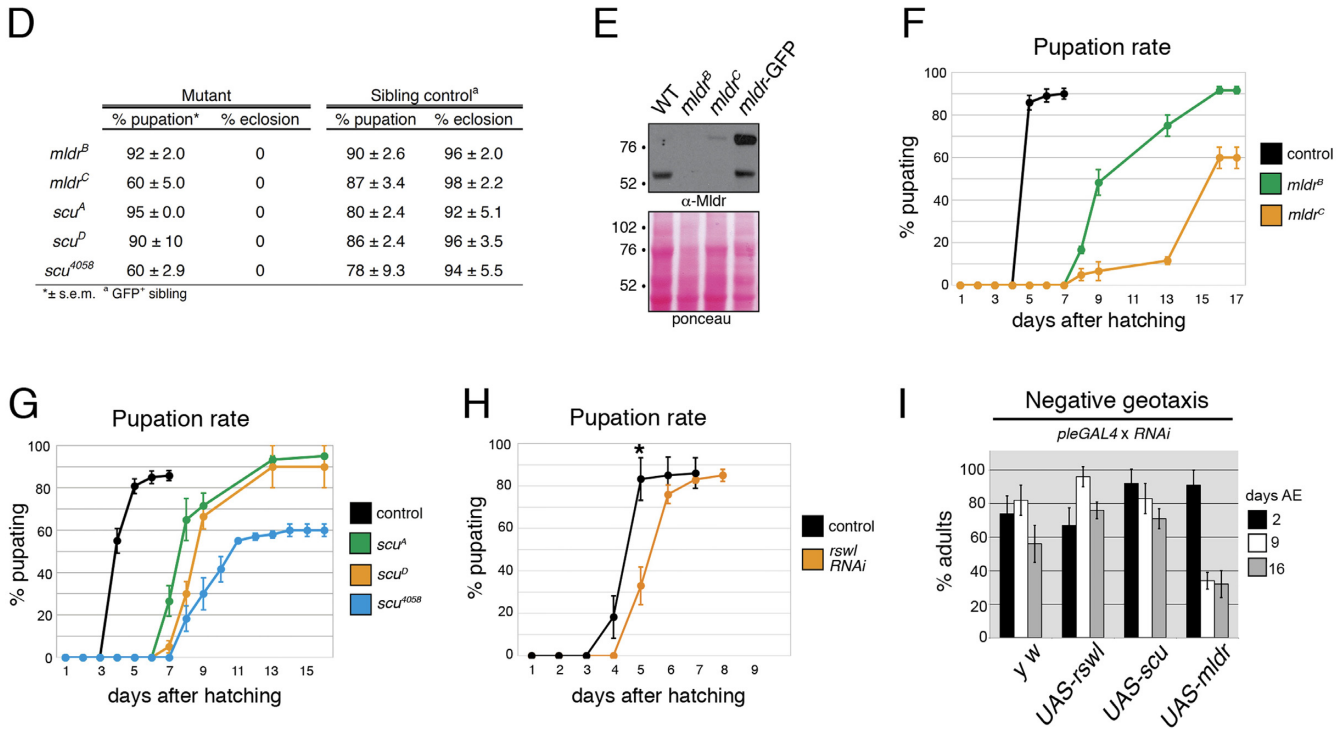

Figure 2. Loss of *mldr* and *scu* results in lethality in Drosophila. (A–C) Predicted structure of Mulder based on the Arabidopsis thaliana PRORP1, PRORP2 and the human PRORP available structures (**A**) and Scully (**B and C**) based on the available human MRPP2 structures. The modeled MRPP2 monomer is shown in blue in B whereas the expected tetrameric assembly is shown in C. The point mutations used in this study are indicated with yellow (A) and red (B, C) circles. The *scu* alleles Q159Stop and E205X result in truncations. The E205X and Q159Stop mutations result in a 19-residue truncation in yellow and an additional 87-residue truncation in green, respectively shown in B. The position of W465, Y121 in Mulder and S163, Q159 and E205 are all shown as ball and sticks. (**D**) Table summarizing percent pupation and eclosion for *mldr* and *scu* alleles. (**E**) Western blot indicating larvae mutant for $mldr^B$ and $mldr^C$ have greatly reduced protein levels. (**F–H**) Pupation rates. Both $mldr^B$ and $mldr^C$ mutant larvae have delayed pupation with 40% of $mldr^C$ mutant larvae failing to pupate (F). Larvae mutant for *scu* have delayed pupation as well. The scu^{4058} allele also fails to pupate 40% of the time (G). (H) Expressing *UAS-rswl-RNAi* using *ActGAL4* shows a modest but reproducible pupation delay. Note the different scale in the X-axis. The controls (black lines) for F–H are a representative sibling control for one of the genotypes. The lines stop because the adults eclose. (**I**) Negative geotaxis assay. Expressing *scu* or *rswl* RNAi in dopaminergic neurons using *Ple-GAL4* has no effect on adult fly locomotion, whereas expressing *mldr-RNAi* causes an age-dependent decrease in locomotion. AE = After Eclosion. Error bars = s.e.m. for F, G and s.d. for H. * $P = 0.02$, determined using a two-tailed Student's *t*-test in Microsoft Excel.

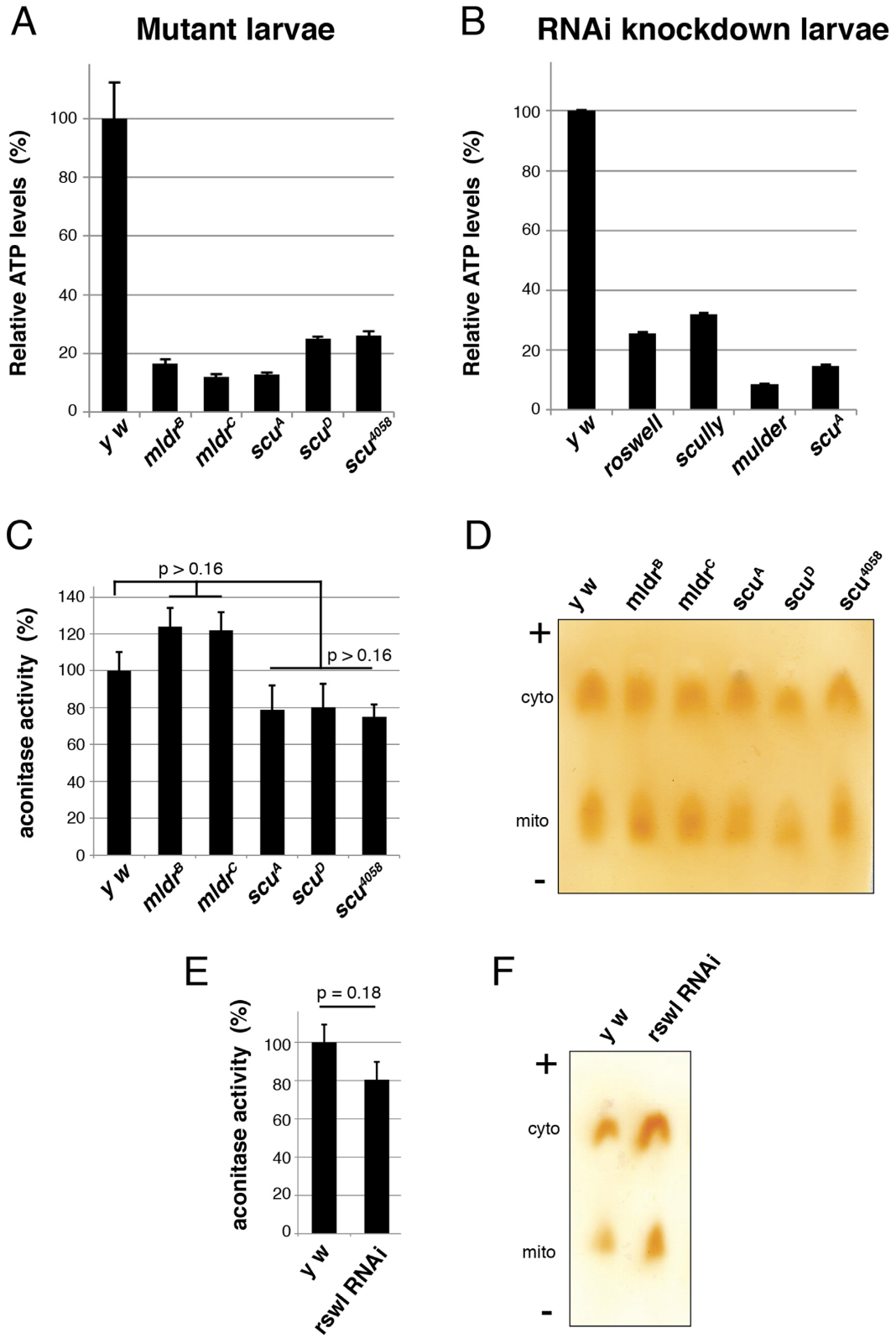

Figure 3. Loss of mt:RNase P complex proteins causes decreases in ATP *in vivo*. (**A**) Larvae mutant for *mldr* and *scu* have greatly reduced levels of ATP compared to wild-type (*y w*). (**B**) Larvae ubiquitously expressing *RNAi* for *rswl*, *scu* and *mldr* using *tubGAL4* also have reduced levels of ATP. scu^{A} mutant larvae are included as a control. (**C, E**) *mldr* and *scu* mutant larvae (C) and larvae ubiquitously expressing *rswl-RNAi* (E) do not have decreased mitochondrial aconitase activity relative to cytoplasmic aconitase activity. (**D, F**) Representative cellulose acetate membranes for C and E, respectively, showing cytoplasmic (cyto) and mitochondrial (mito) aconitase activity. '+' and '–' indicate the electrophoretic migration. Error bars represent s.e.m.. *P*-values were calculated using a two-tailed Student's *t*-test in Microsoft Excel. Information on replicates can be found in the Materials and Methods.

Table 1. mt:RNase P *RNAi* knockdown pupation and eclosion rates

	RNAi		Sibling control[b]	
	Percent pupation[a]	Percent eclosion	Percent pupation	Percent eclosion
tubGAL4/ UAS-rswl^{GD12447}	0	0	85 ± 5	98 ± 1.8
ActGAL4/ UAS-rswl^{GD12447}	92 ± 3.3	0	98 ± 1.7	98 ± 1.7
UAS-scu$^{TRiP.HMS02305}$ /+; *tubGAL4*/+	86 ± 7.2	0	98 ± 2.5	98
tubGAL4/ UAS-scu$^{TRiP.GL01079}$	92 ± 1.7	0	95 ± 2.9	97 ± 3.3
tubGAL4/ UAS-mldr^{KK108043}	83 ± 1.7	8 ± 5.1	92 ± 1.7	97 ± 3.3

[a]± s.e.m.
[b]GFP^+ sibling larvae.

tion of reactive oxygen species. If reactive oxygen species accumulate, mitochondria can experience a reduction in ATP due to the build-up of general oxidative damage as a consequence of oxidative stress. For example, Drosophila harboring mutations for various mitochondrial proteins often suffer from mitochondrial oxidative damage and flies lacking mt:RNase Z function were shown to have increased oxidative damage (examples include (29,40–43)). One assay to assess the mitochondrial redox environment is to measure the enzymatic ability of mitochondrial aconitase, an enzyme easily rendered non-functional due to oxidation (44,45). *mldr* and *scu* mutants and *rswl RNAi* knockdown larvae did not show a decrease in mitochondrial aconitase activity relative to cytoplasmic aconitase activity (Figure 3C–F). This suggests that the drop in ATP levels is not due to general mitochondrial oxidative stress.

Mitochondria swell in the absence of Mldr and Scu

When the inner mitochondrial membrane of a mitochondrion loses its selective permeability due to damage, it osmotically swells and ruptures the outer mitochondrial membrane. This phenomenon gives rise to swollen, ring-like mitochondria when viewed by microscopy. Mldr, Scu and Rswl localized to mitochondria, and there was a decrease in ATP levels when any of the three were knocked down. The lethality we observed with *mldr* and *scu* mutants and with *UAS-rswl-RNAi* knockdown could be due to a variety of non-specific defects. To examine whether there are defects in mitochondrial size and shape with loss of mt:RNase P, we examined mitochondrial morphology using immunofluorescence. Mitochondria in larval brain neuroblasts have a stereotypical, distinctive, small spherical structure (Figure 4A) (29). When we examined neuroblasts in *mldr* and *scu* mutant larval brains, we found they were larger and swollen compared to wild-type, and often contained ring-like mitochondria (Figure 4C–G, arrows, versus A). For *scu*^{4058}, this is consistent with mitochondrial morphological changes seen using transmission electron microscopy (32). Loss of mitochondrial proteins in Drosophila does not always give rise to this phenotype (29). In contrast, the *rswl RNAi* knockdown using tubGAL4 did not show swollen or ring-like mitochondria, even though these larvae do not grow past second instars (Figure 4B).

Mitochondrial tRNA processing is altered in the absence of Mldr and Scu

Products encoded by mtDNA do not contain introns and with the exception of the A+T rich region, there are very few nucleotides that do not encode mRNA, rRNA or tRNA (Figure 5A) (27). Drosophila mtDNA is thought to be transcribed as five polycistrons (5,6). tRNAs in these polycistronic units are thought to serve as punctuation marks for 3′ and 5′ end processing of mitochondrial rRNAs and mRNAs (8). As such, most mt:mRNAs and mt:rRNAs are separated by at least one mt:tRNA (Figure 5A). Since the human mt:RNase P complex cleaves the mt:tRNA 5′-ends *in vitro*, we investigated whether mt:tRNA processing was aberrant *in vivo* in *mldr* and *scu* mutants and with *rswl RNAi* knockdown. mt:tRNAs are found in different sequence milieux. To test a variety of upstream sequence context, we chose to examine tRNAs that are found downstream of rRNA (mt:tRNA$^{Leu(CUN)}$ and mt:tRNA^{Val}), mRNA (Cytochrome c oxidase subunit III (CoIII), mt:tRNA^{Gly}) and the A+T rich region (mt:tRNA^{Ile}) (Figure 5A, asterisks). mt:tRNA processing by Arabidopsis PRORPs appears to be highly efficient and go to completion at steady-state levels *in vitro* (46); thus, normally unprocessed tRNAs would not be predicted to be observable by northern analysis. As such, wild-type larvae consistently and completely processed each of the mt:tRNAs we examined, with no evidence of unprocessed higher molecular weight RNA intermediates (Figure 5B–E, *y w*). In contrast, the mutant alleles of *mldr* and *scu*, and the larvae expressing *rswl RNAi* knockdown accumulated precursor mitochondrial RNAs (Figure 5B–E). mt:tRNA^{Ile} and mt:tRNA^{Gly} are encoded in the same polycistron. After probing for mt:tRNA^{Ile} in *mdlr* mutants, we observed three distinct bands, in contrast to *scu* mutants and *rswl RNAi* knockdown. Probing for mt:tRNA^{Gly}, however, showed only a single band (Figure 5C). mt:tRNA$^{Leu(CUN)}$ and mt:tRNA^{Val} are in the same polycistron and when probing with each gave bands at approximately the same sizes for *mldr* and *scu* mutants and *rswl* knockdown.

Overexpressing Mldr causes mitochondrial dysfunction

For multiprotein enzyme complexes, a decrease in any one protein often results in changes or loss of enzymatic function. Mutations in *mldr* and *scu*, as well as *RNAi* knockdown of *rswl*, resulted in pupal death, developmental delays and a decrease in mitochondrial function indicating each is essential *in vivo*. On the other hand, ectopically increasing enzyme levels can also lead to dominant negative effects through sequestering critical components from their normal function, or through mis-regulated activity. Using *tubGAL4* for high, global expression, we found overexpressing *UAS-mldr-GFP* and *UAS-rswl-myc* resulted in

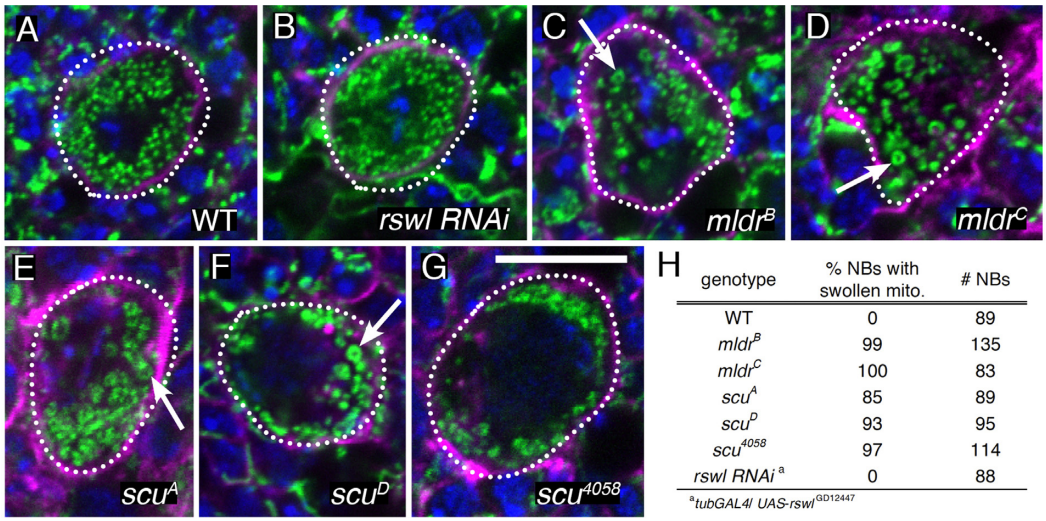

H

genotype	% NBs with swollen mito.	# NBs
WT	0	89
mldr^{B}	99	135
mldr^{C}	100	83
scu^{A}	85	89
scu^{D}	93	95
scu^{4058}	97	114
rswl RNAi [a]	0	88

[a] *tubGAL4/ UAS-rswl*^{GD12447}

Figure 4. Larvae lacking Mldr and Scu have mitochondrial defects. (**A–G**) Larval stem cells (dashed circles) from third instar larval brains labeled for mitochondria (green), actin (magenta) and DAPI (blue). Larval stem cells in wild-type brains have small, dispersed mitochondria (A). (**C–G**) In contrast, mitochondria in the neuroblasts of *mldr* and *scu* mutants are grossly swollen with frequent ring-shaped mitochondria (arrows). (B) Ubiquitously expressing *rwsl*-RNAi using *tubGAL4* does not cause defects in mitochondrial morphology. (**H**) Table indicating the penetrance of neurobasts (NB) with swollen mitochondria and the number of neuroblasts examined. Green = anti-ATP synthase, magenta = phalloidin, blue = DAPI (A–G). Scale bar = 10 μm in G for A–G.

lethality (Table 2). Larvae overexpressing *mldr* could develop to second instars, but often did not develop past first instar (Figure 6A). In contrast, larvae overexpressing *rswl* were able to develop to third instars (Figure 6B). In agreement with the lethality, both genotypes exhibited low levels of ATP production (Figure 6C). Larvae overexpressing *scu* had increased ATP levels relative to *mldr* and *rswl*, albeit lower than wild-type, which did not result in lethality (Figure 6C, Table 2). To determine whether mitochondrial morphology was affected, we examined germ cells. *nanos-GAL4* (*nosGAL4*) is expressed exclusively in the germline. The *nosGAL4* stock we used does not give uniform expression in all developmental stages of the ovary, with lower expression in early germ cells and very high expression later (Figure 6J). When we examined mitochondrial morphology using immunofluorescence, we observed that in the lower expressing germ cells, mitochondria had the narrow, rod-shaped morphology characteristic of normal germ cell mitochondria (Figure 6D–F). However, mitochondria in germ cells with high expression of *UAS-mldr* had swollen, ring-shaped mitochondria indicative of a loss of selective permeability (Figure 6G–I). ATP synthase, which is found in the mitochondrial inner-membrane, labeled the outside of the ring-shaped mitochondria (Figure 6H, inset) whereas antibodies against Mldr, which is a mitochondrial matrix protein, labeled the inside of the mitochondrial rings (Figure 6G and I). Although overexpressing *UAS-rswl-myc* ubiquitously was lethal and decreased ATP levels, in contrast to *UAS-mldr*, mitochondrial morphology was normal (Figure 1I–K, Supplementary Figure S4). These results indicate that past a threshold expression level, Mldr causes dominant effects.

DISCUSSION

Each component of mt:RNase P is required *in vivo*

PRORPs represent a new class of tRNA 5′-end processing enzymes that lack a catalytic RNA component, i.e. a ribozyme. In humans, PRORP requires the obligatory presence of a sub-complex containing MRPP1 and MRPP2 to catalyze the cleavage reaction. The complex was initially identified from mitochondrial extracts and while it has been localized to mitochondria in cell culture, the physiological significance of these proteins during development has not been previously addressed *in vivo* (47). Here, we have shown that Drosophila contains orthologs of each member of the mt:RNase P complex: Mulder (PRORP), Scully (MRPP2) and Roswell (MRPP1). Each member localizes to mitochondria, and its loss causes lethality. In addition, decreasing the amount of Mldr, Scu or Rswl causes an accumulation of unprocessed mt:tRNAs, supporting that they function in the mt:tRNA processing pathway and that the mitochondrial defects seen in the mutants (loss of ATP, mitochondrial morphology defects) may be due to a decrease in mature mt:tRNAs.

Mldr levels are the most critical *in vivo*

Overall, the lethality we observed in *mldr* and *scu* mutants and *rswl RNAi* knockdown was very similar and consistent. All were pupal lethal, and *mldr* and *scu* mutants showed delayed pupation. Even though *mldr*^{B} and *mldr*^{C} are point mutations, there are low levels of protein present (Figure 2E). While both alleles cause a lack of protein, *mldr*^{C} (W465R) has a more severe developmental defect since 40% of the larvae do not pupate, suggesting that there is a difference in how any potential residual protein functions between the two alleles. The *scu* mutants we examined also showed differences in lethality, with *scu*^{4058} being the most severe

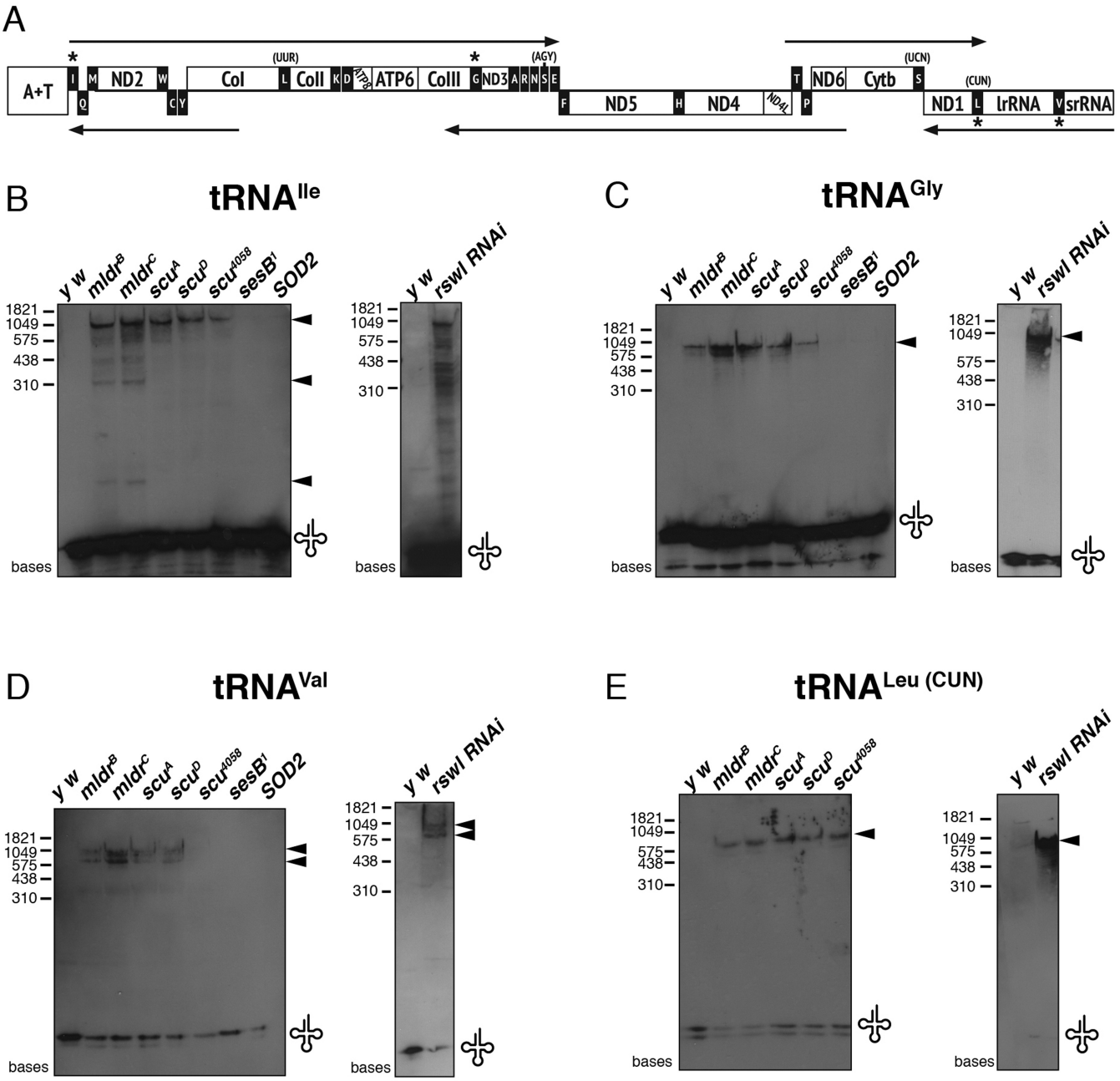

Figure 5. The mt:RNase P complex is required for mt:tRNA processing in Drosophila. (**A**) Diagram of Drosophila mitochondrial DNA structure (adapted from Xie and Dubrovsky). The five arrows indicate the predicted five transcribed polycistrons. Asterisks denote which mt:tRNAs were assayed via northern blot. ND = NADH dehydrogenase (Complex I), Cytb = ubiquinol: cytochrome c oxidoreductase (Complex III), Co = Cytochrome c oxidase (Complex IV), ATP = ATP synthase (Complex V). (B–E) Northern blots. *mldr* and *scu* mutant larvae contain unprocessed mt:tRNAs transcripts for mt:tRNA^{Ile}, mt:tRNA^{Gly}, mt:tRNA^{Val} and mt:tRNA$^{Leu(CUN)}$. Northern blots using extract from *rswl RNAi* knockdown larvae also show unprocessed, larger molecular weight species. Arrows indicate the major additional bands. *sesB^1* and *SOD2* mutant larvae are used as controls. The mature tRNAs are indicated by the tRNA symbol at the bottom of the blot.

which is surprising given that *scu^A* is a larger truncation. One potential explanation is that the additional amino acids left in *scu^{4058}* allows it to sequester other proteins, acting as a dominant negative. The human MRPP2 ortholog must form a tetramer in order to function (48,49). The truncations for *scu^{4058}* and *scu^A*, shown in only the blue monomer in Figure 2C, and color-coded with two lighter shades of blue, form the majority of the dimerization interface. It seems that even if these truncations were to result in viable coded proteins they would be unable to form a tetramer. Thus, it is likely these *scu* mutations could lead to disruption of tetramer formation with subsequent detrimental effects to the mt:RNase P function. In addition, MRPP2 (also known as HSD10 (HSD17B10 is the gene)) is known to function in the isoleucine biosynthetic pathway. However, patients suffering from HSD10 disease have symptoms that

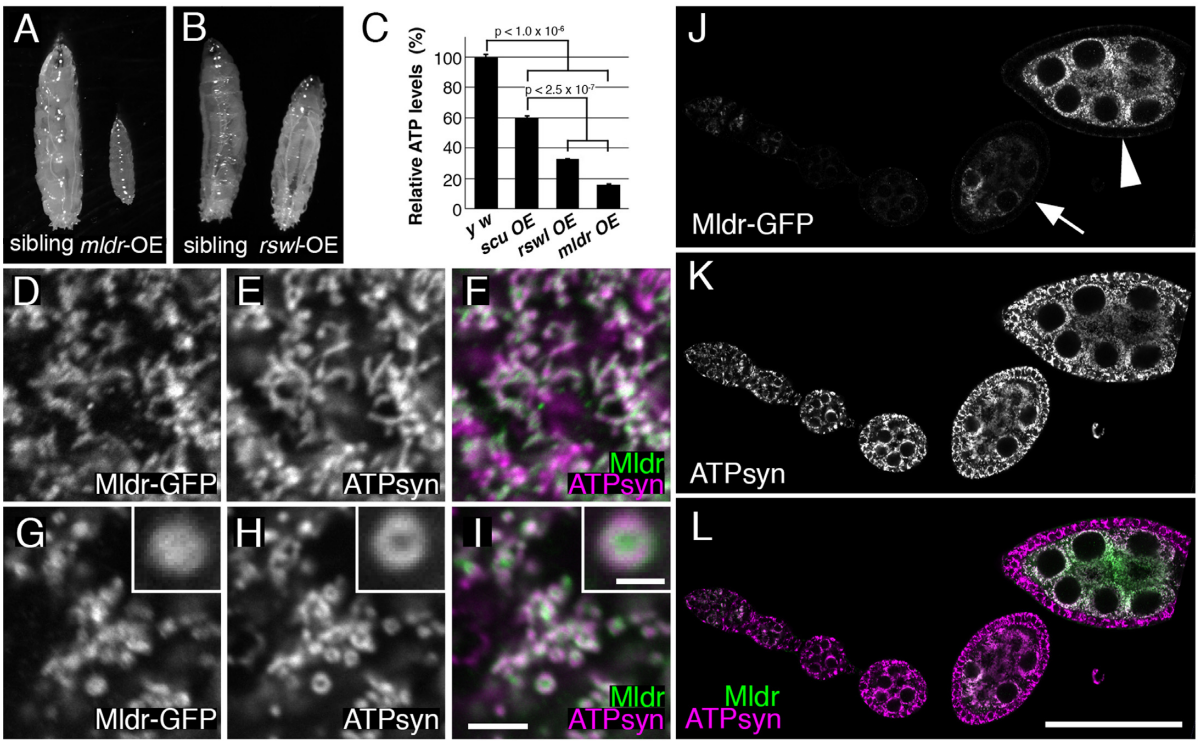

Figure 6. Overexpressing Mulder causes mitochondrial morphology defects. (**A**) *UAS-mldr-GFP* expressing larvae driven by *tubGAL4* do not develop past second instar. The sibling control larva is a third instar. (**B**) *UAS-rswl-myc* larvae, in contrast, are able to grow to the third instar stage driven by *tubGAL4*. (**C**) Graph showing relative ATP levels for *UAS-scu*, *UAS-rswl* and *UAS-mldr* larvae overexpressed using *tubGAL4*. OE = overexpression. (**D–I**) Germ cells expressing *UAS-mldr-GFP* under the control of *nosGAL4*. (D–F) Germ cells with lower Mldr expression (D) have mitochondria that are of the normal shape and size (E, F is the merge). Germ cells with high expression of UAS-Mldr-GFP (G) have swollen mitochondria (H, I is the merge). The swollen, ring-shaped mitochondria (H, inset) have Mldr-GFP concentrated in the middle (G, inset, I inset is the merge). (**J–L**) A representative ovariole expressing *UAS-mldr-GFP* under control of *nosGAL4*. Weaker expression is seen in younger germ cells (J, arrow) compared to strong Mldr-GFP expression in older ones (J, arrowhead). ATP synthase labeling shows all of the mitochondria throughout the ovariole (K). L is the merge of J and K. White = anti-GFP (D, G, J), anti-ATP synthase (E, H, K). Green = anti-GFP (F, I, L). Magenta = anti-ATP synthase (F, I, L). Scale bars = 5 μm in I for D-I, 1.5 μm in I inset for all insets, 50 μm in L for J–L. Error bars = s.e.m.. *P*-values were calculated in Microsoft Excel using a two-tailed Student's *t*-test.

Table 2. Effect of mt:RNase P overexpression

tubGAL4/ TM3 Ser ActGFP x	Number of adults	
	Balancer	non-Balancer
UAS-rswl-myc-4a/Y	299[a]	0
UAS-rswl-myc-5a/TM3 Sb	163	3
UAS-rswl-myc-1b/CyO	167	1
UAS-scu-FLAG-3a	300	327
UAS-scu-FLAG-3a/CyO[b]	168	70
UAS-scu-FLAG-4a/CyO	199	84
UAS-mldr-GFP-4b	213	0
UAS-mldr-GFP-2a/TM6b Hu Tb	125	0
UAS-mldr-GFP-4a/Y	108[a]	0

[a]includes all males.
[b]same insertion as 3a, maintained as a balanced stock.

do not correlate with an increase in toxic metabolites due to misregulated isoleucine biosynthesis. Rather, the symptoms are related to mitochondrial dysfunction and apoptotic cell death (50). Thus, while MRPP2/HSD10 has dehydrogenase activity, it is likely the loss of mitochondrial function associated with *MRPP2/HSD17B10* mutations is primarily due to its non-enzymatic function in the mt:RNase P.

In addition to the common phase of lethality, knockdown of *mldr*, *scu* and *rswl* exhibited greatly reduced ATP levels and accumulation of unprocessed mt:RNAs (Figures 3 and 5). However, our more detailed analyses of mitochondrial function revealed some critical differences between the three proteins. For example, only *mldr RNAi* caused an age-related decrease in locomotion when expressed in dopaminergic neurons (Figure 2I). In addition, *mldr* and *scu* mutants had swollen and ring-like mitochondria in neuroblasts, whereas *rswl-RNAi* did not (Figure 4). In general, when mitochondria have this morphology, it is indicative of a loss of selective permeability. Once this is lost, the mitochondrial outer membrane fragments, leading to a lack of ATP production. However, normal morphology does not necessarily mean ATP production is at appropriate levels.

These data suggest that while all three proteins are essential, cells are most sensitive to reductions in Mldr.

Interestingly, while decreasing Mldr, Scu and Rswl caused lethality, overexpressing Mldr and Rswl had the same effect (Table 2). In contrast, overexpressing *UAS-scu-FLAG* in a wild-type background resulted in the expected Mendelian ratio of adults, suggesting that too much of Scu does not appear to alter the function of the complex, cause a deleterious increase in dehydrogenase activity or sequester any critical components in a dominant negative fashion. In contrast, overexpressing Mldr was lethal, led to decreased ATP levels and also caused defects in mitochondrial morphology (Figure 6). Overexpressing Rswl was lethal, but unlike Mldr, did not appear to change mitochondrial morphology as judged by immunofluorescence (Supplementary Figure S4). One possible explanation is that too much Mldr causes indiscriminate nucleotide cleavage in the mitochondrion resulting in a more severe effect. However, while the lethal outcome of Rswl overexpression may be more specific to mt:tRNA processing, we cannot rule out there is a concomitant deleterious increase in nonselective methyltransferase activity. It could be that an increase in indiscriminate methyltransferase activity is simply not as deleterious as nucleotide cleavage while still being important. Thus, decreasing and increasing Rswl expression causes a decrease in ATP and lethality, but does not give rise to any mitochondrial morphological changes. Looking at all of the phenotypes caused by lack and overexpression of the three mt:RNase P complex members, it is apparent based on our data that Drosophila is most sensitive to alterations in the levels of Mldr.

Decreasing Drosophila mt:RNase P complex proteins does not cause oxidative stress

We saw a consistent loss of ATP for *mldr* and *scu* mutants, as well as RNAi knockdown of *mldr*, *scu* and *rswl*. The ATP loss is very striking, and is not necessarily observed in other larvae mutant for proteins involved in various mitochondrial functions (29,43). However, we observed no accompanying oxidative stress by assaying mitochondrial aconitase function. Mitochondrial aconitase is well established as being exceedingly sensitive to oxidation, and thus loss of its function is often used as an indirect assay for an increased mitochondrial oxidative environment (45,51). Mutating Drosophila proteins involved in mitochondrial function does not always lead to oxidative stress in larvae (29). One possible reason is that since mitochondria fulfill a variety of biochemical functions, lowering levels of different pathways would not necessarily cause oxidative stress. Another possible reason is that there is evidence that larvae primarily use glycolysis, and not respiration, to maintain ATP levels (52). Respiration is primarily responsible for generating reactive oxygen species in mitochondria since the electron transport chain can be 'leaky'.

RNAse Z is the enzyme responsible for 3′-end tRNA cleavage. Drosophila lacking mitochondrial RNAse Z have been reported to have cell cycle defects, as well as oxidative damage (43). In contrast, we did not observe any particularly small imaginal disks (indicative of cell cycle defects), and while larvae development showed a delay, the larval brains were of relatively normal size, as were the pupae that formed. It is still possible that mutant clones would be smaller relative to their wild-type siblings. Thus, it appears that while flies lacking either mt:RNAse Z or mt:RNase P accumulate unprocessed mitochondrial RNA species, they have different effects on ATP levels and oxidative stress (43).

Reducing Mldr, Scu and Rswl results in accumulation of unprocessed mitochondrial RNAs

Larvae mutant for *mldr* and *scu*, as well as *rswl RNAi* knockdown, accumulate unprocessed mt:RNAs (Figure 5). There are several conclusions that can be gleaned from these experiments. Wild-type larvae consistently and completely processed the four mt:tRNAs we examined, as did the $sesB^{1}$ and *SOD2* mutants – two genes mutated in unrelated processes (53–55). Thus, accumulation of mt:RNAs was specific for Mldr, Scu and Rswl and not due to general mitochondrial dysfunction. For mt:tRNA^{Ile} and mt:tRNA^{Gly}, which are encoded in the polycistron downstream of the A + T rich region, the amount of processed mt:tRNA was larger compared to mt:tRNA^{Val} and mt:tRNA$^{Leu(CUN)}$, both encoded in the polycistron that also encodes the large and small mt:rRNAs. There are several possible explanations for this observation. First, both ribozyme and protein-only RNase P enzymes have differential affinities and cleavage rates for some RNA substrates *in vitro* (46,56–58). Thus the differences in the amount of processed product could be due to different cleavage efficiencies of mt:RNase P for the two polycistrons. However, given that there is more processed product for mt:tRNA^{Ile} and mt:tRNA^{Gly}, the two polycistrons would also need to be differentially transcribed, as happens in humans (59). Since the same amount of total RNA was added for all the blots, it is possible the two polycistrons are differentially transcribed. However, counterintuitively, the polycistron encoding the mt:rRNAs appears to be at lower levels than the one downstream of the A + T rich region, in contrast to what is thought to happen for human mtDNA (59). The difference in transcript levels does not appear to be due to non-specific binding of the probes to other tRNAs, as performing BLAST analysis with each full-length mt:tRNA probe (Supplementary Table S2) did not recognize any other tRNAs. Alternatively, this could be explained by differences in probe binding, however, the unprocessed mt:mRNAs were of similar intensity for all the blots.

In addition, $mldr^{C}$ mutant larvae had the largest accumulation of unprocessed mt:tRNAs. This is consistent with it being the more severe *mldr* allele, as well as with our observations that Drosophila are most sensitive to perturbation in Mldr levels. For mt:tRNA^{Ile} processing, *mldr* mutants showed several band sizes of unprocessed mt:tRNAs, which may reflect the potential influence of *mldr* mutations on the specificity of the 5′ end cleavage (Figure 5B). In contrast, the *scu* mutations affected mt:tRNA^{Ile} 5′-end processing of the same cleavage sites equally. *rswl RNAi* also showed a variety of band sizes for mt:tRNA^{Ile} cleavage. By size, these bands cannot be clearly associated with putative RNA transcripts including tRNA^{Ile}. It is possible that these detected bands are products of miscleavage by Rswl deficient mt:RNase P,

suggesting a potential role of Rswl in restricting substrate recognition.

mt:RNase P and disease

Many mitochondrial diseases are associated with point mutations in mtDNA (60). While mt:tRNAs encode for a relatively small proportion of mtDNA, over 50% of the disease-causing mutations found in mtDNA are found in the mt:tRNAs (61). However, most of these mt:tRNA mutations do not occur in the anticodon or discriminator bases that are necessary for codon recognition and aminoacylation. Therefore, these disease-causing mt:tRNA mutations likely impact such processes as post-transcriptional modifications, interaction with the translation machinery or mt:tRNA processing. There is evidence that normal mt:tRNA processing is critical as mutations in precursor mt:tRNAs that impair mt:tRNA 5′-end maturation, as well as in human PRORP, can give rise to disease (19–20,23,62). Studying how loss of Mldr, Scu or Rswl function affects cellular function is therefore important for promoting the understanding of the mechanisms of these mitochondrial diseases.

SUPPLEMENTARY DATA

Supplementary Data are available at NAR Online.

ACKNOWLEDGEMENTS

We would like to thank Drs Frank Shewmaker and Xin Xiang for critically reading the manuscript. We would also like to thank the USU Biomedical Instrumentation Core. The Drosophila Genomics Resource Center, supported by NIH grant 2P40OD010949-10A1, provided reagents. Stocks obtained from the Bloomington Drosophila Stock Center (NIH P40OD018537) and Vienna Drosophila Resource Center were used in this study.

FUNDING

National Institutes of Health [1R01GM117141 to M.K.]; Uniformed Services University [USUHS BIO-71-3019 to R.T.C.]; National Institutes of Health/Department of Defense [CHIRP HU0001-14-2-0041 to R.T.C.]. Funding for open access charge: NIH R01 GM117141.
Conflict of interest statement. None declared.

REFERENCES

1. Gissi,C., Iannelli,F. and Pesole,G. (2008) Evolution of the mitochondrial genome of Metazoa as exemplified by comparison of congeneric species. *Heredity (Edinb.)*, **101**, 301–320.
2. Jackman,J.E. and Alfonzo,J.D. (2013) Transfer RNA modifications: nature's combinatorial chemistry playground. *Wiley Interdiscip. Rev. RNA*, **4**, 35–48.
3. Paris,Z., Fleming,I.M. and Alfonzo,J.D. (2012) Determinants of tRNA editing and modification: avoiding conundrums, affecting function. *Semin. Cell Dev. Biol.*, **23**, 269–274.
4. Phizicky,E.M. and Hopper,A.K. (2010) tRNA biology charges to the front. *Genes Dev.*, **24**, 1832–1860.
5. Berthier,F., Renaud,M., Alziari,S. and Durand,R. (1986) RNA mapping on Drosophila mitochondrial DNA: precursors and template strands. *Nucleic Acids Res.*, **14**, 4519–4533.
6. Torres,T.T., Dolezal,M., Schlotterer,C. and Ottenwalder,B. (2009) Expression profiling of Drosophila mitochondrial genes via deep mRNA sequencing. *Nucleic Acids Res.*, **37**, 7509–7518.
7. Mercer,T.R., Neph,S., Dinger,M.E., Crawford,J., Smith,M.A., Shearwood,A.M., Haugen,E., Bracken,C.P., Rackham,O., Stamatoyannopoulos,J.A. *et al.* (2011) The human mitochondrial transcriptome. *Cell*, **146**, 645–658.
8. Ojala,D., Montoya,J. and Attardi,G. (1981) tRNA punctuation model of RNA processing in human mitochondria. *Nature*, **290**, 470–474.
9. Hartmann,R.K., Gossringer,M., Spath,B., Fischer,S. and Marchfelder,A. (2009) The making of tRNAs and more - RNase P and tRNase Z. *Progress Mol. Biol. Translat. Sci.*, **85**, 319–368.
10. Rossmanith,W. (2012) Of P and Z: mitochondrial tRNA processing enzymes. *Biochim. et Biophys. Acta*, **1819**, 1017–1026.
11. Guerrier-Takada,C., Gardiner,K., Marsh,T., Pace,N. and Altman,S. (1983) The RNA moiety of ribonuclease P is the catalytic subunit of the enzyme. *Cell*, **35**, 849–857.
12. Holzmann,J., Frank,P., Löffler,E., Bennett,K.L., Gerner,C. and Rossmanith,W. (2008) RNase P without RNA: identification and functional reconstitution of the human mitochondrial tRNA processing enzyme. *Cell*, **135**, 462–536.
13. Gobert,A., Gutmann,B., Taschner,A., Gossringer,M., Holzmann,J., Hartmann,R.K., Rossmanith,W. and Giege,P. (2010) A single Arabidopsis organellar protein has RNase P activity. *Nat. Struct. Mol. Biol.*, **17**, 740–744.
14. Taschner,A., Weber,C., Buzet,A., Hartmann,R.K., Hartig,A. and Rossmanith,W. (2012) Nuclear RNase P of Trypanosoma brucei: a single protein in place of the multicomponent RNA-protein complex. *Cell Reports*, **2**, 19–25.
15. Vilardo,E., Nachbagauer,C., Buzet,A., Taschner,A., Holzmann,J. and Rossmanith,W. (2012) A subcomplex of human mitochondrial RNase P is a bifunctional methyltransferase–extensive moonlighting in mitochondrial tRNA biogenesis. *Nucleic Acids Res.*, **40**, 11583–11593.
16. Brzezniak,L.K., Bijata,M., Szczesny,R.J. and Stepien,P.P. (2011) Involvement of human ELAC2 gene product in 3′ end processing of mitochondrial tRNAs. *RNA Biol.*, **8**, 616–626.
17. Suzuki,T., Nagao,A. and Suzuki,T. (2011) Human mitochondrial tRNAs: biogenesis, function, structural aspects, and diseases. *Annu. Rev. Genet.*, **45**, 299–329.
18. Bindoff,L.A., Howell,N., Poulton,J., McCullough,D.A., Morten,K.J., Lightowlers,R.N., Turnbull,D.M. and Weber,K. (1993) Abnormal RNA processing associated with a novel tRNA mutation in mitochondrial DNA. A potential disease mechanism. *J. Biological Chem.*, **268**, 19559–19564.
19. Chatfield,K.C., Coughlin,C.R. 2nd, Friederich,M.W., Gallagher,R.C., Hesselberth,J.R., Lovell,M.A., Ofman,R., Swanson,M.A., Thomas,J.A., Wanders,R.J. *et al.* (2015) Mitochondrial energy failure in HSD10 disease is due to defective mtDNA transcript processing. *Mitochondrion*, **21**, 1–10.
20. Deutschmann,A.J., Amberger,A., Zavadil,C., Steinbeisser,H., Mayr,J.A., Feichtinger,R.G., Oerum,S., Yue,W.W. and Zschocke,J. (2014) Mutation or knock-down of 17beta-hydroxysteroid dehydrogenase type 10 cause loss of MRPP1 and impaired processing of mitochondrial heavy strand transcripts. *Hum. Mol. Genet.*, **23**, 3618–3628.
21. Li,R. and Guan,M.X. (2010) Human mitochondrial leucyl-tRNA synthetase corrects mitochondrial dysfunctions due to the tRNALeu(UUR) A3243G mutation, associated with mitochondrial encephalomyopathy, lactic acidosis, and stroke-like symptoms and diabetes. *Mol. Cell. Biol.*, **30**, 2147–2154.
22. Rossmanith,W. and Karwan,R.M. (1998) Characterization of human mitochondrial RNase P: novel aspects in tRNA processing. *Biochem. Biophys. Res. Commun.*, **247**, 234–241.
23. Wang,S., Li,R., Fettermann,A., Li,Z., Qian,Y., Liu,Y., Wang,X., Zhou,A., Mo,J.Q., Yang,L. *et al.* (2011) Maternally inherited essential hypertension is associated with the novel 4263A>G mutation in the mitochondrial tRNAIle gene in a large Han Chinese family. *Circ. Res.*, **108**, 862–870.
24. Haack,T.B., Kopajtich,R., Freisinger,P., Wieland,T., Rorbach,J., Nicholls,T.J., Baruffini,E., Walther,A., Danhauser,K., Zimmermann,F.A. *et al.* (2013) ELAC2 mutations cause a

mitochondrial RNA processing defect associated with hypertrophic cardiomyopathy. *Am. J. Hum. Genet.*, **93**, 211–223.
25. Vilardo,E. and Rossmanith,W. (2015) Molecular insights into HSD10 disease: impact of SDR5C1 mutations on the human mitochondrial RNase P complex. *Nucleic Acids Res.*, **43**, 5112–5119.
26. Yarham,J.W., Elson,J.L., Blakely,E.L., McFarland,R. and Taylor,R.W. (2010) Mitochondrial tRNA mutations and disease. *Wiley Interdiscip. Rev. RNA*, **1**, 304–324.
27. Lewis,D.L., Farr,C.L. and Kaguni,L.S. (1995) Drosophila melanogaster mitochondrial DNA: completion of the nucleotide sequence and evolutionary comparisons. *Insect. Mol. Biol.*, **4**, 263–278.
28. Dietzl,G., Chen,D., Schnorrer,F., Su,K.C., Barinova,Y., Fellner,M., Gasser,B., Kinsey,K., Oppel,S., Scheiblauer,S. *et al.* (2007) A genome-wide transgenic RNAi library for conditional gene inactivation in Drosophila. *Nature*, **448**, 151–156.
29. Sen,A., Damm,V.T. and Cox,R.T. (2013) Drosophila clueless is highly expressed in larval neuroblasts, affects mitochondrial localization and suppresses mitochondrial oxidative damage. *PLoS One*, **8**, e54283.
30. Sen,A., Kalvakuri,S., Bodmer,R. and Cox,R.T. (2015) Clueless, a protein required for mitochondrial function, interacts with the PINK1-Parkin complex in Drosophila. *Dis. Model Mech.*, **8**, 577–589.
31. Schneider,C.A., Rasband,W.S. and Eliceiri,K.W. (2012) NIH Image to ImageJ: 25 years of image analysis. *Nat. Methods*, **9**, 671–675.
32. Torroja,L., Ortuno-Sahagun,D., Ferrus,A., Hammerle,B. and Barbas,J.A. (1998) scully, an essential gene of Drosophila, is homologous to mammalian mitochondrial type II L-3-hydroxyacyl-CoA dehydrogenase/amyloid-beta peptide-binding protein. *J. Cell Biol.*, **141**, 1009–1017.
33. Brand,A.H. and Perrimon,N. (1993) Targeted gene expression as a means of altering cell fates and generating dominant phenotypes. *Development*, **118**, 401–415.
34. Kelley,L.A., Mezulis,S., Yates,C.M., Wass,M.N. and Sternberg,M.J. (2015) The Phyre2 web portal for protein modeling, prediction and analysis. *Nat. Protoc.*, **10**, 845–858.
35. Li,F., Liu,X., Zhou,W., Yang,X. and Shen,Y. (2015) Auto-inhibitory mechanism of the human mitochondrial RNase P protein complex. *Sci. Rep.*, **5**, 9878.
36. Reinhard,L., Sridhara,S. and Hallberg,B.M. (2015) Structure of the nuclease subunit of human mitochondrial RNase P. *Nucleic Acids Res.*, **43**, 5664–5672.
37. Lustbader,J.W., Cirilli,M., Lin,C., Xu,H.W., Takuma,K., Wang,N., Caspersen,C., Chen,X., Pollak,S., Chaney,M. *et al.* (2004) ABAD directly links Abeta to mitochondrial toxicity in Alzheimer's disease. *Science*, **304**, 448–452.
38. Yang,J., Yan,R., Roy,A., Xu,D., Poisson,J. and Zhang,Y. (2015) The I-TASSER Suite: protein structure and function prediction. *Nature Methods*, **12**, 7–8.
39. Haelterman,N.A., Jiang,L., Li,Y., Bayat,V., Sandoval,H., Ugur,B., Tan,K.L., Zhang,K., Bei,D., Xiong,B. *et al.* (2014) Large-scale identification of chemically induced mutations in Drosophila melanogaster. *Genome Res.*, **24**, 1707–1718.
40. Kirby,K., Hu,J., Hilliker,A.J. and Phillips,J.P. (2002) RNA interference-mediated silencing of Sod2 in Drosophila leads to early adult-onset mortality and elevated endogenous oxidative stress. *Proc. Natl. Acad. Sci. U S A*, **99**, 16162–16167.
41. Macchi,M., El Fissi,N., Tufi,R., Bentobji,M., Lievens,J.C., Martins,L.M., Royet,J. and Rival,T. (2013) The Drosophila inner-membrane protein PMI controls crista biogenesis and mitochondrial diameter. *J. Cell. Sci.*, **126**, 814–824.
42. Sandoval,H., Yao,C.K., Chen,K., Jaiswal,M., Donti,T., Lin,Y.Q., Bayat,V., Xiong,B., Zhang,K., David,G. *et al.* (2014) Mitochondrial fusion but not fission regulates larval growth and synaptic development through steroid hormone production. *Elife*, **3**, e03558.
43. Xie,X. and Dubrovsky,E.B. (2015) Knockout of Drosophila RNase ZL impairs mitochondrial transcript processing, respiration and cell cycle progression. *Nucleic Acids Res.*, **43**, 10364–10375.
44. Flint,D.H., Tuminello,J.F. and Emptage,M.H. (1993) The inactivation of Fe-S cluster containing hydro-lyases by superoxide. *J. Biol. Chem.*, **268**, 22369–22376.
45. Gardner,P.R. and Fridovich,I. (1991) Superoxide sensitivity of the *Escherichia coli* aconitase. *J. Biol. Chem.*, **266**, 19328–19333.
46. Howard,M.J., Karasik,A., Klemm,B.P., Mei,C., Shanmuganathan,A., Fierke,C.A. and Koutmos,M. (2016) Differential substrate recognition by isozymes of plant protein-only Ribonuclease P. *RNA*, **22**, 782–792.
47. Sanchez,M.I., Mercer,T.R., Davies,S.M., Shearwood,A.M., Nygard,K.K., Richman,T.R., Mattick,J.S., Rackham,O. and Filipovska,A. (2011) RNA processing in human mitochondria. *Cell Cycle*, **10**, 2904–2916.
48. Kissinger,C.R., Rejto,P.A., Pelletier,L.A., Thomson,J.A., Showalter,R.E., Abreo,M.A., Agree,C.S., Margosiak,S., Meng,J.J., Aust,R.M. *et al.* (2004) Crystal structure of human ABAD/HSD10 with a bound inhibitor: implications for design of Alzheimer's disease therapeutics. *J. Mol. Biol.*, **342**, 943–952.
49. Powell,A.J., Read,J.A., Banfield,M.J., Gunn-Moore,F., Yan,S.D., Lustbader,J., Stern,A.R., Stern,D.M. and Brady,R.L. (2000) Recognition of structurally diverse substrates by type II 3-hydroxyacyl-CoA dehydrogenase (HADH II)/amyloid-beta binding alcohol dehydrogenase (ABAD). *J. Mol. Biol.*, **303**, 311–327.
50. Rauschenberger,K., Scholer,K., Sass,J.O., Sauer,S., Djuric,Z., Rumig,C., Wolf,N.I., Okun,J.G., Kolker,S., Schwarz,H. *et al.* (2010) A non-enzymatic function of 17beta-hydroxysteroid dehydrogenase type 10 is required for mitochondrial integrity and cell survival. *EMBO Mol. Med.*, **2**, 51–62.
51. Gardner,P.R., Nguyen,D.D. and White,C.W. (1994) Aconitase is a sensitive and critical target of oxygen poisoning in cultured mammalian cells and in rat lungs. *Proc. Natl Acad. Sci. U.S.A.*, **91**, 12248–12252.
52. Tennessen,J.M., Baker,K.D., Lam,G., Evans,J. and Thummel,C.S. (2011) The Drosophila estrogen-related receptor directs a metabolic switch that supports developmental growth. *Cell Metabol.,* **13**, 139–148.
53. Celotto,A.M., Frank,A.C., McGrath,S.W., Fergestad,T., Van Voorhies,W.A., Buttle,K.F., Mannella,C.A. and Palladino,M.J. (2006) Mitochondrial encephalomyopathy in Drosophila. *J. Neurosci.*, **26**, 810–820.
54. Fergestad,T., Bostwick,B. and Ganetzky,B. (2006) Metabolic disruption in Drosophila bang-sensitive seizure mutants. *Genetics*, **173**, 1357–1364.
55. Zhang,Y.Q., Roote,J., Brogna,S., Davis,A.W., Barbash,D.A., Nash,D. and Ashburner,M. (1999) stress sensitive B encodes an adenine nucleotide translocase in Drosophila melanogaster. *Genetics*, **153**, 891–903.
56. Liu,F. and Altman,S. (1994) Differential evolution of substrates for an RNA enzyme in the presence and absence of its protein cofactor. *Cell*, **77**, 1093–1100.
57. Sugita,C., Komura,Y., Tanaka,K., Kometani,K., Satoh,H. and Sugita,M. (2014) Molecular characterization of three PRORP proteins in the moss Physcomitrella patens: nuclear PRORP protein is not essential for moss viability. *PLoS One*, **9**, e108962.
58. Koutmou,K.S., Zahler,N.H., Kurz,J.C., Campbell,F.E., Harris,M.E. and Fierke,C.A. (2010) Protein-precursor tRNA contact leads to sequence-specific recognition of 5′ leaders by bacterial ribonuclease P. *J. Mol. Biol.*, **396**, 195–208.
59. Terzioglu,M., Ruzzenente,B., Harmel,J., Mourier,A., Jemt,E., Lopez,M.D., Kukat,C., Stewart,J.B., Wibom,R., Meharg,C. *et al.* (2013) MTERF1 binds mtDNA to prevent transcriptional interference at the light-strand promoter but is dispensable for rRNA gene transcription regulation. *Cell Metabol.*, **17**, 618–626.
60. Wallace,D.C. (1992) Diseases of the mitochondrial DNA. *Annual Rev. Biochem.*, **61**, 1175–1212.
61. Ruiz-Pesini,E., Lott,M.T., Procaccio,V., Poole,J.C., Brandon,M.C., Mishmar,D., Yi,C., Kreuziger,J., Baldi,P. and Wallace,D.C. (2007) An enhanced MITOMAP with a global mtDNA mutational phylogeny. *Nucleic Acids Res.*, **35**, D823–D828.
62. Rossmanith,W. and Karwan,R.M. (1998) Impairment of tRNA processing by point mutations in mitochondrial tRNA(Leu)(UUR) associated with mitochondrial diseases. *FEBS Lett.*, **433**, 269–274.